Eur. Phys. J. E **16**, 89–96 (2005)
DOI: 10.1140/epje/e2005-00011-4

THE EUROPEAN PHYSICAL JOURNAL E

Memory effects in vibrated granular systems: Response properties in the generalized random sequential adsorption model

L.J. Budinski-Petković[1] and S.B. Vrhovac[2,a]

[1] Faculty of Engineering, Trg D. Obradovića 6, Novi Sad 21000, Serbia and Montenegro
[2] Institute of Physics, P.O. Box 68, Zemun 11080, Belgrade, Serbia and Montenegro

Received 29 July 2004
Published online 31 January 2005 –

Abstract. We investigate, by numerical simulation, the dynamical response of a granular system to an abrupt change in shaking intensity within the framework of the reversible random sequential adsorption models. We analyse the two-dimensional lattice model in which, in addition to the adsorption-desorption process, there is diffusion of the adsorbed particles on the surface. Our model reproduces qualitatively the densification kinetics and the memory effects of vibrated granular materials. An interpretation of the simulation results is provided by the analysis of the insertion probability function. The importance of the diffusional relaxation is discussed. We conclude that a complex time-evolution of the density could be explained as a consequence of the variation of the diffusion rate during the compaction. We study the nonequilibrium time-dependent density-density autocorrelation function and show that the model displays out-of-equilibrium dynamical effects such as aging.

PACS. 45.70.Cc Static sandpiles; granular compaction – 82.20.Wt Computational modeling; simulation – 81.05.Rm Porous materials; granular materials

1 Introduction

Dense granular media are complex disordered systems, which exhibit many fascinating properties such as slow density relaxation, annealing properties and hysteresis effects [1,2]. The phenomenon of granular compaction involves the increase of the density of a granular medium subjected to shaking, tapping or, more generally, to some kind of external excitation. This problem is of fundamental importance to many industrial applications and also raises some fundamental theoretical questions. The compaction has been extensively analyzed in a series of experiments by the Chicago group [1–3], that suggested that the density, $\rho(t)$, follows an inverse logarithmic law with the tapping number, $\rho(\infty)-\rho(t) \sim 1/\ln(t)$. The final density, $\rho(\infty)$, is a monotonic decreasing function of the dimensionless vibration intensity, $\Gamma = A/g$, where A is the peak acceleration in a tap, and g is the gravity. Moreover, the slope of the relaxation curve is smaller for smaller vibration intensity, Γ, i.e. the relaxation is slower for smaller Γ.

The phenomenology of the granular compaction is very rich, showing many characteristic glassy behaviors. Here we will focus on one of them, namely on the response of the granular system to sudden perturbations of the 'effective temperature' given by Γ. Recently, it has been shown [4] that, during the compaction, the response to an abrupt change in the tapping acceleration, Γ, is opposite to what could be expected from the long-time behavior of the compaction. For a sudden decrease in Γ it was observed that on short-time scales the compaction rate increases, while for a sudden increase in Γ the system dilates for short times. This behavior is however transient, and after several taps the usual compaction rate is recovered. Recently, Nicolas et al. [5] have also shown that periodic shear compaction exhibits a nontrivial response to a sudden change in shear amplitude. The rapid variation of volume fraction induced by the sudden change of shear angle is proportional and opposite to the angle change.

In the last few years, a series of models has been proposed to identify the physical principles underlying the granular compaction. Most of the studies have been performed for (off-lattice) adsorption-desorption or parking lot model [2,6–11], frustrated lattice gas models [12–17] and one-dimensional lattice models with short-range dynamical constraints [18–22]. These models, despite their apparent simplicity, are able to reproduce many features of real granular materials: slow density relaxation [6–8,16,18], density fluctuations [2,6,7], aging [9,13,16,17], hysteresis [9,20] and memory effects [9–12,17,21]. The study of simple models has been very useful in order to understand, at least qualitatively, the glassylike behavior of dense granular systems, but a complete and detailed physical theory (or reference model) of the densification process is still lacking.

We study the phenomenon of the granular compaction within the framework of the well-known class

[a] e-mail: vrhovac@phy.bg.ac.yu

of lattice-based models, the so-called reversible Random Sequential Adsorption (RSA) model with diffusional relaxation [23,24]. In this paper we discuss how reversible RSA on two-dimensional lattices with diffusional relaxation may be used to describe the dynamical response of the granular system to perturbations of shaking amplitudes. In particular, we explore the behavior of the model for abrupt changes in the diffusion rate, that were not considered before. Finally, we study the nonequilibrium two-time density-density correlation function $C(t, t_0)$ and find aging effects typical for glassy systems. We focus, in particular, on the influence of diffusion on the decay of $C(t, t_0)$.

The phenomenon of compaction results from the existence of packing defects, such as voids, in a randomly packed granular material. When mechanical energy is supplied to a powder, in the form of shaking, periods of release are introduced. During the periods of release, the grains and voids have some freedom to rearrange their positions relative to their neighbors. The waiting time between successive taps is large enough to allow the system to relax, so that the initial state for each tap is the final state from the previous relaxation. The consecutive repetition of both processes, tapping and free evolution, reduces the porosity of the material and makes it denser.

This physical situation corresponds to the events occurring in reversible RSA with diffusional relaxation [23]. This model can be regarded as a simple picture of a horizontal slice or layer of a real granular material, parallel to the bottom of the container. In the reversible RSA, objects are placed in a space of arbitrary dimension at randomly selected positions with constant rate k_+. If the trial position does not result in an overlap with a previously placed object, a new object is accepted. In addition, all adsorbed objects are subjected to removal (desorption) at random with a constant rate k_-. Motivated by the theoretical [24] and experimental work [3], we use the two-dimensional lattice-based model in which the previously deposited objects are allowed to diffuse on the layer. The diffusion of a deposited particle is attempted in a randomly selected direction on the surface with constant rate k_d. The particle moves along the selected direction if it finds a space large enough to accommodate in. Some partial analyses of this model have already been reported [25,26]. We note that Tarjus et al. [24] have considered the diffusional relaxation of a continuum irreversible RSA problem.

This paper is organized as follows. In Section 2 the model is introduced. Section 3 is devoted to the analysis of the short-term memory effects by considering the response of the system to the abrupt change in the desorption and diffusion rate. Finally, Section 4 contains some additional comments and final remarks.

2 Definition of the model and the simulation method

A square lattice of size 120×120 represents a given layer of the material and the adsorbing objects are squares of size 2×2, covering four lattice sites. The periodic boundary conditions are used in both directions.

The tapping processes are modeled in our lattice system in the following way. At each Monte Carlo step adsorption is attempted with probability $P_+ = 1$, desorption with probability P_- and diffusion with probability P_d. These processes are essentially independent and they are performed simultaneously. For each of these processes a lattice site is selected at random. In the case of adsorption, we try to place the object with the fixed point (say the left upper corner of the object) at the selected site, checking whether all relevant sites are unoccupied. If the selected site is occupied by the fixed point of a previously adsorbed object and if the attempted process is desorption, the object is removed from the layer. On the other hand, when the attempted process is diffusion, we choose one of the four possible directions at random and try to move the object for a lattice constant in that direction. The object is moved if it does not overlap with any of the previously deposited objects; if it does, the attempt is abandoned. Hence, the desorption process is unrestricted while the adsorption and diffusion is subjected to free volume constraints, i.e. two objects cannot overlap.

The time t is counted by the number of adsorption attempts and scaled by the total number of lattice sites, L^2. If we assume that one tapping event corresponds to one adsorption attempt per lattice site, the time is actually measured in the number of tapping events.

The kinetics of the process is governed by the ratios of adsorption to desorption rate (k_+/k_-) and adsorption to diffusion rate (k_+/k_d). In our model these ratios correspond to the ratios of adsorption/desorption probability ($K = 1/P_-$) and adsorption/diffusion probability ($R = 1/P_d$). In our model the ratio $1/K$ plays a role similar to the intensity of vibration, Γ, in real experiments. In our simulation, we will analyze the influence of the other parameter, R, i.e. diffusion, on the relaxation of the density.

At certain time t_0 instantaneous changes in the desorption or diffusion probabilities are made. The changes in the vibration intensity, Γ, correspond to the changes of the desorption probability, P_-. The data are averaged over 100 independent runs for each combination of desorption and diffusion probabilities.

3 Monte Carlo results and discussion

In this section we present the results of the simulations for the previously described model subject to abrupt changes in the desorption and diffusion probabilities.

The kinetics of the adsorption-desorption model has been previously investigated for large but finite values of K [24–27]. In the limit of small desorption rate the densification is extremely slow: a logarithmic regime, where the density varies as $1/\ln(t)$, persists until the density is very close to the equilibrium value. We restrict ourselves to this stage, because the logarithmic part of the relaxation process corresponds to the experimentally observed behavior of vibrated granular materials. In the final regime,

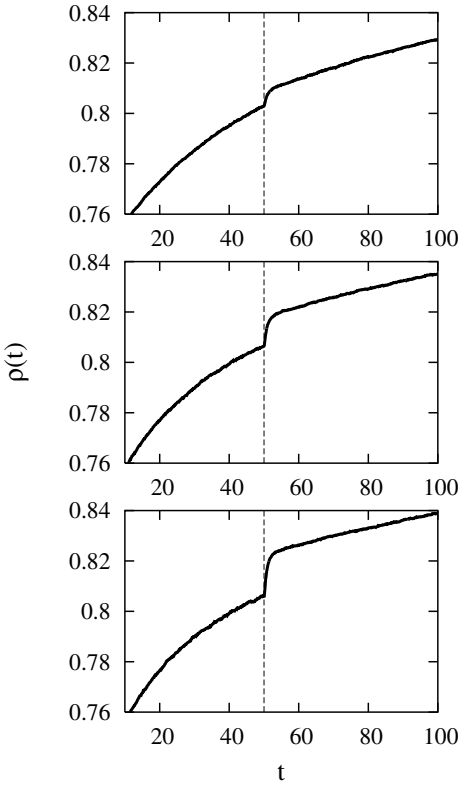

Fig. 1. Time evolution of the density, ρ, when the desorption probability is changed at $t_0 = 50$, from $P_-^{(1)} = 0.02,\ 0.03,\ 0.04$ to $P_-^{(2)} = 0.01$, from top to bottom. Other parameters: $P_+ = 1$, and $P_d = 0.01$.

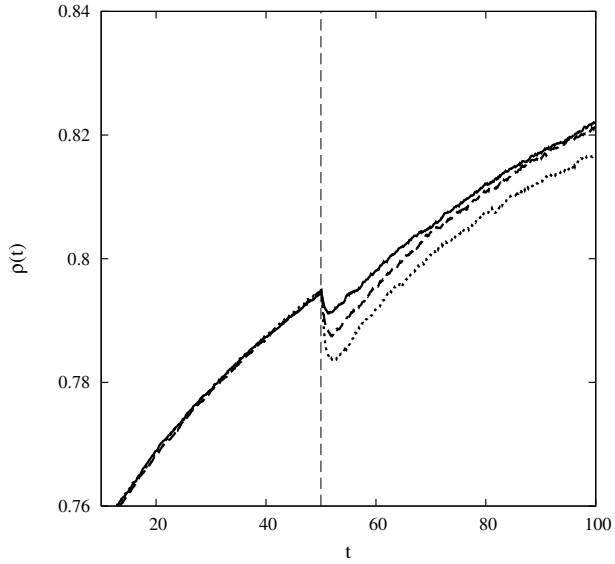

Fig. 2. Time evolution of the density, ρ, when the desorption probability is changed at $t_0 = 50$, from $P_-^{(1)} = 0.01$ to $P_-^{(2)} = 0.02$ (solid), 0.03 (dashed), and 0.04 (doted). Other parameters: $P_+ = 1$, and $P_d = 0.01$.

the rate of desorption events becomes comparable to the rate of adsorption events, and an exponential approach to an equilibrium disordered state occurres. In the presence of diffusion, the rearrangement of the layer is more rapid and the equilibrium is reached more quickly for greater diffusion probabilities, P_d. However, the equilibrium coverage depends only on the desorption/adsorption probability ratio. The possibility of diffusion always fastens the relaxation of the system. The impact of diffusion is the most important for low desorption rates [26].

In order to mimic what is done in the recent experiments [4] with real granular materials we proceed in the following way. Starting from an empty lattice, the system evolves at a fixed desorption and diffusion probability, $P_-^{(1)}$ and P_d. We always use the adsorption probability of value 1, $P_+ = 1$. At a certain time, $t_0 = 50$, desorption probability changes from $P_-^{(1)}$ to another value $P_-^{(2)}$. For $P_-^{(1)} > P_-^{(2)}$ ($\Gamma_1 > \Gamma_2$) we find that the compaction rate increases on short-time scales (Fig. 1). For $P_-^{(1)} < P_-^{(2)}$ ($\Gamma_1 < \Gamma_2$) we observe a short-term memory effect opposite to the previous case (Fig. 2). We find that the change in the compaction rate has an opposite sign to that of the change in the vibration intensity. The comparison of the density relaxations at various changes in the tapping acceleration (at fixed P_d and t_0) shows that the amplitude of the jump in the compaction rate is larger for larger jump of desorption probability. These results are in agreement with the experimental results, but are contrary to our expectations that would stem from the compaction behavior at constant forcing.

The interpretation of these results is quite straightforward using the results of [6,8,26]. The compaction rate just before t_0 is determined by vibration intensity $\Gamma(t_0-0)$ ($P_-(t_0-0)$) and by the fraction of the substrate, $\Phi(t_0-0)$, that is available for the insertion of a new particle. As can be seen from Figure 3, the quantity $\Phi(t_0-0)$ (the insertion probability) strongly depends on the *state* of the system, but it is not unambiguously determined by the density $\rho(t_0-0)$ at the same instant. When Γ (P_-) is abruptly lowered, the first effect is that the particles tend to decrease the fraction of the substrate that is available for deposition of new particles, and the layer becomes more compact. Therefore the rate of compaction first increases with respect to the unperturbed case. At larger times, however, the compaction is slowed down by the creation of a denser substrate and smaller fraction of the layer that is available for the insertion of a new particle.

When the tapping intensity Γ (P_-) is suddenly increased at t_0, the first effect is decompaction. On short-time scales, the interplay between the insertion probability and adsorption/desorption probability ratio leads to the fast density changes. During this transient stage the fraction of the substrate that is available for the insertion of a new particle is an increasing function of time. After this transient interval, the adsorption events prevail, and the compaction proceeds faster. The growing of the insertion probability, $\Phi(t)$, during the transient time leads to more efficient densification afterwards.

In order to demonstrate the short-term memory effects in a more explicit manner, we have also considered another series of numerical experiments where the system

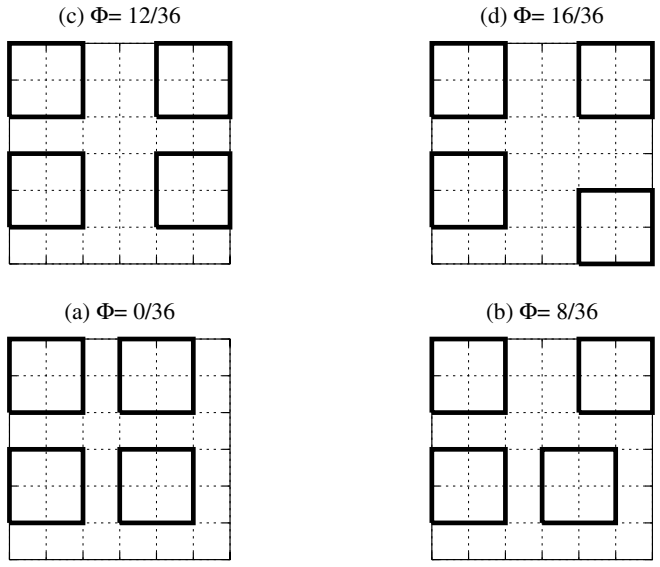

Fig. 3. Schematic representation of different coverings on square lattice of size 6×6 sites. The adsorbing objects are squares covering 4 lattice sites. Periodic boundary conditions are used in all directions. All four coverigs have the same density, $\rho_0 = 16/36$, but different values of insertion probability $\Phi = 0/36$ (a), $8/36$ (b), $12/36$ (c), $16/36$ (d).

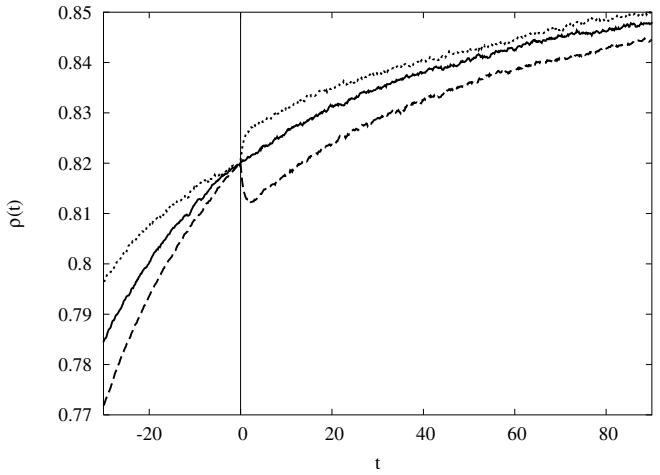

Fig. 4. Time evolution of the density ρ for a system which was compacted up to the same density, $\rho_0 = 0.82$, using three different desorption probabilities (vibration intensities), $P_-^{(1)} = 0.04$ (doted), 0.03 (solid), 0.01 (dashed). After the coverage $\rho_0 = 0.82$ was achieved, the system was always tapped with $P_-^{(2)} = 0.03$. The time origin for each curve has been taken at the time when the system reached the prescribed density $\rho_0 = 0.82$. The evolution for $t > 0$ strongly depends on the prehistory of the system.

was tapped to the same density $\rho_0 = 0.82$ with three different vibration intensities Γ_0 ($P_-^{(0)} = 0.03$), Γ_1 ($P_-^{(1)} = 0.01$) and Γ_2 ($P_-^{(2)} = 0.04$). After the density ρ_0 was achieved, the system was always tapped with the same intensity, Γ_0. The time evolution of the density is shown in Figure 4, where the time origin for each experiment has been taken

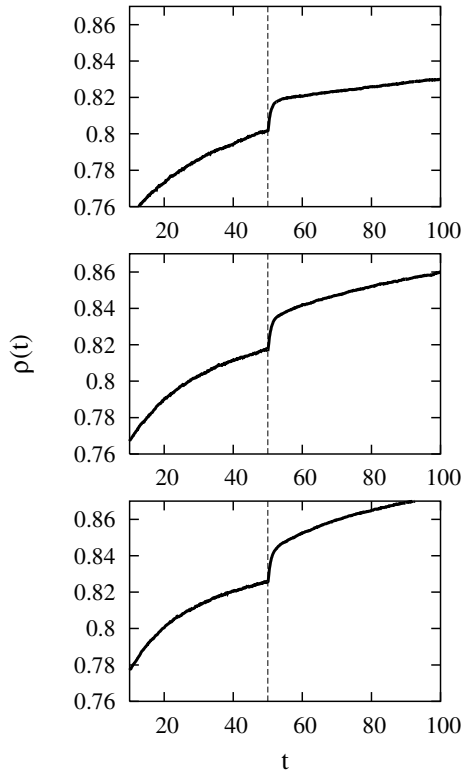

Fig. 5. Time evolution of the density, ρ, for three different diffusion probabilities, $P_d = 0,\ 0.05,\ 0.10$, from top to bottom. The desorption probability was changed at $t_0 = 50$, from $P_-^{(1)} = 0.04$ to $P_-^{(2)} = 0.01$. Other parameter: $P_+ = 1$.

at the time when the system reached the prescribed density ρ_0. The figure clearly shows that the three systems prepared at the same density but in different ways display different behaviors if the same tapping acceleration is applied to them. In other words, the density after the perturbation of the vibration intensities depends not only on the density ρ_0, but also on the previous tapping history. The memory of the history up to the density ρ_0 is encoded in the arrangement of the deposited objects on the lattice. In our numerical experiment, we have constructed three different packing topologies corresponding to the same density ρ_0, each one with different value of insertion probability Φ. Since the systems with different values of the insertion probability respond in different ways to the tapping, it is obvious to conclude that at the microscopical level, the information about the past history is encoded in the values of the insertion probability.

An interesting behavior of the system is also revealed in response properties when, in addition, we investigate the influence of diffusion. Figures 5 and 6 show typical memory effects at short times after an abrupt change of the desorption probability, P_-, for *different* values of diffusion probability $P_d = 0,\ 0.05,\ 0.10$. Desorption probability P_- is switched from 0.01 to 0.04 and vice versa at $t_0 = 50$. We observe that after several adsorption/desorption events (or taps) the 'anomalous' response ceases and there is a crossover to the 'normal' behavior, with the relaxation rate becoming the same as in constant forcing mode.

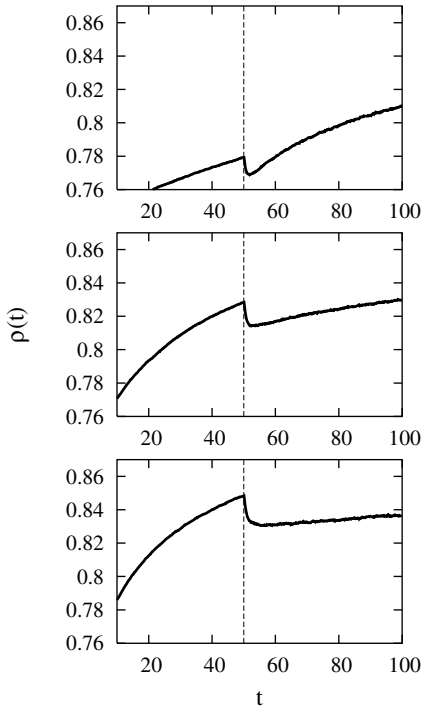

Fig. 6. Time evolution of the density, ρ, for three different diffusion probabilities, $P_d = 0,\ 0.05,\ 0.10$, from top to bottom. The desorption probability is changed at $t_0 = 50$, from $P_-^{(1)} = 0.01$ to $P_-^{(2)} = 0.04$. Other parameter: $P_+ = 1$.

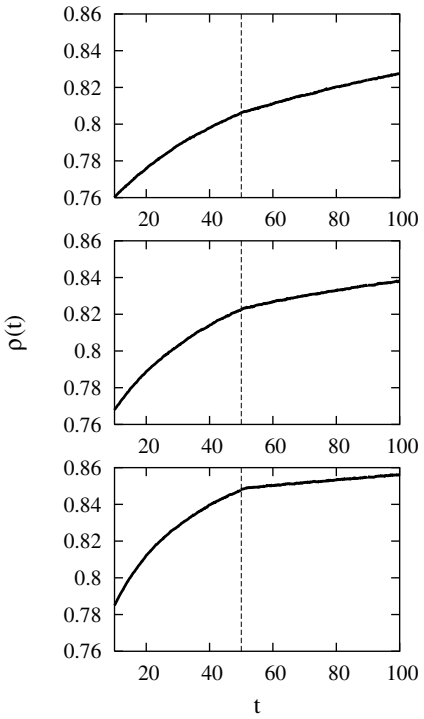

Fig. 7. Time evolution of the density, ρ, when the diffusion probability is changed at $t_0 = 50$, from $P_d^{(1)} = 0.02,\ 0.04,\ 0.10$ to $P_d^{(2)} = 0.01$, from top to bottom. Other parameters: $P_- = 0.01$, and $P_+ = 1$.

However, the difference between the value of compaction rate just before the change in the intensity of vibration at instant t_0 and the value of compaction rate just after the transient period strongly depends on diffusion probability. From Figures 5 and 6, it follows that the jump in the compaction rate is less pronounced as P_d increases.

We have also studied the effect of an abrupt change in the diffusion probability P_d on the densification kinetics with constant desorption probability P_-. This is illustrated in Figures 7 and 8. We observe that the variation of the compaction rate has the same sign as the change in diffusion probability. For completeness, in Figure 9 we show the response of the system to the diffusion probability shift from $P_d^{(1)} = 0.01$ to $P_d^{(2)} = 0.05$ at a time $t_0 = 50$ for several values of desorption probability: $P_- = 0.01,\ 0,02,\ 0.04$. We find that the impact of the sudden increase in the diffusion probability is the most evident for low desorption rates. For sufficiently small desorption probabilities, diffusion is rapid enough to significantly modify the surface configuration between two consecutive adsorption/desorption events. After one adsorption/desorption event, the configuration on the surface evolves rapidly at constant density, changing significantly the insertion probability function, Φ, on the timescale of the order of the characteristic time for desorption. These rearrangements of the adsorbed objects on the layer always accelerate the compaction of the layer [26].

We have also examined the time correlation functions in order to obtain a comprehensive information about the

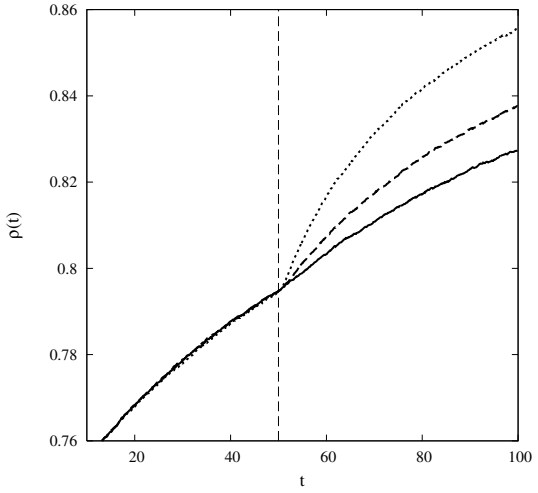

Fig. 8. Time evolution of the density, ρ, when the diffusion probability is changed at $t_0 = 50$, from $P_d^{(1)} = 0.01$ to $P_d^{(2)} = 0.02$ (solid), 0.04 (dashed), and 0.10 (doted). Other parameters: $P_- = 0.01$, and $P_+ = 1$.

out-of-equilibrium dynamics in our system. Specifically, we have evaluated the two-time density-density correlation function, $C(t, t_0)$, and qualitatively analyzed its dependence on diffusion processes. The normalized two-time density-density correlation function is defined as follows,

$$C(t, t_0) = \frac{\langle \rho(t)\rho(t_0)\rangle - \langle \rho(t)\rangle \langle \rho(t_0)\rangle}{\langle \rho^2(t_0)\rangle - \langle \rho(t_0)\rangle^2}, \quad t \geq t_0, \qquad (1)$$

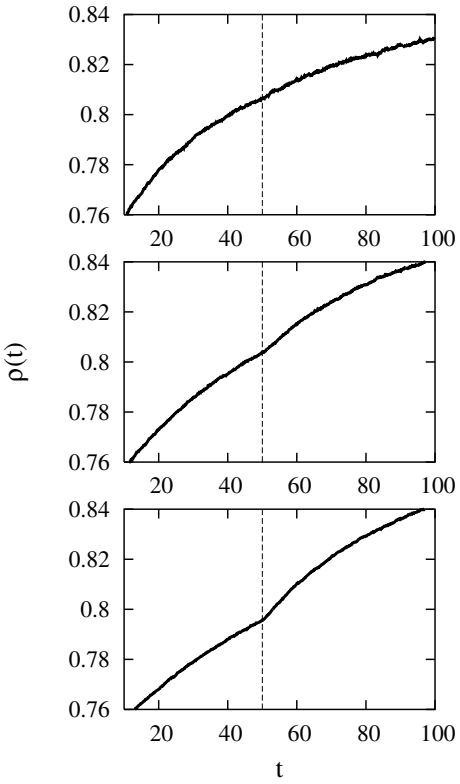

Fig. 9. Time evolution of the density, ρ, for three different desorption probabilities, $P_- = 0.04,\ 0.02,\ 0.01$, from top to bottom. The diffusion probability is changed at $t_0 = 50$, from $P_d^{(1)} = 0.01$ to $P_d^{(2)} = 0.05$. Other parameter: $P_+ = 1$.

where the angular brackets denote an average over independent runs. In order to obtain reasonable statistics, it is necessary to average over many independent runs (typically 10^4). Out of equilibrium, $C(t, t_0)$ is a function of both times, t and t_0.

Figure 10 shows the influence of the diffusion on the decay of $C(t, t_0)$, after instantaneous change in the desorption probability at time $t_0 = 50$. At short times, the decay of $C(t, t_0)$ is fast. The first relaxation step consists of 'fast' rearrangements on the layer with an appreciable influence of diffusion processes. In the next relaxation step, the decay curves have similar shapes for all values of P_d. The global properties of the correlation function depend smoothly on the diffusion probability: as P_d grows, the correlation decays faster, as shown in Figure 10. However, the correlation curves do not differ qualitatively and they have similar shapes.

In Figure 11 we show the behavior of $C(t, t_0)$ for several values of the waiting time t_0. We observe the typical ageing behavior: the larger t_0, the longer memory of the initial state persists. The aging properties of the system are characterized by specific scaling properties of $C(t, t_0)$. In the Tetris and Ising frustrated lattice gas models, it was found that the relaxation of the $C(t, t_0)$ is given by the form [13]:

$$C(t, t_0) = (1 - c_\infty)\frac{\ln[(t_0 + t_s)/\tau]}{\ln[(t + t_s)/\tau]} + c_\infty, \qquad (2)$$

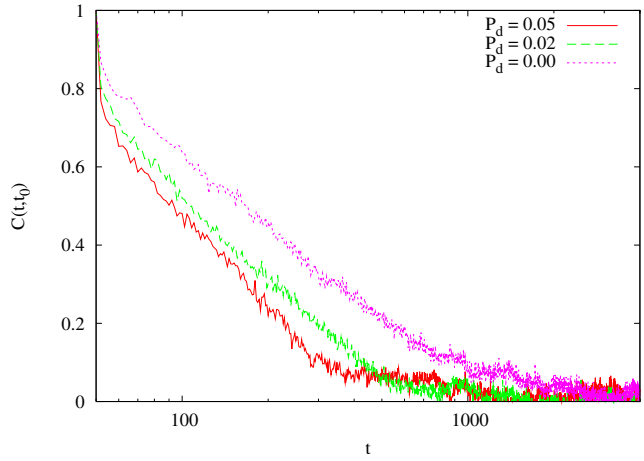

Fig. 10. (Color online) Two-time density-density correlation function as a function of time, for $t_0 = 50$, and three values of diffusion probability, $P_d = 0$ (doted), 0.02 (dashed) and 0.05 (solid). Other parameters: $P_+ = 1$, and $P_- = 0.01$.

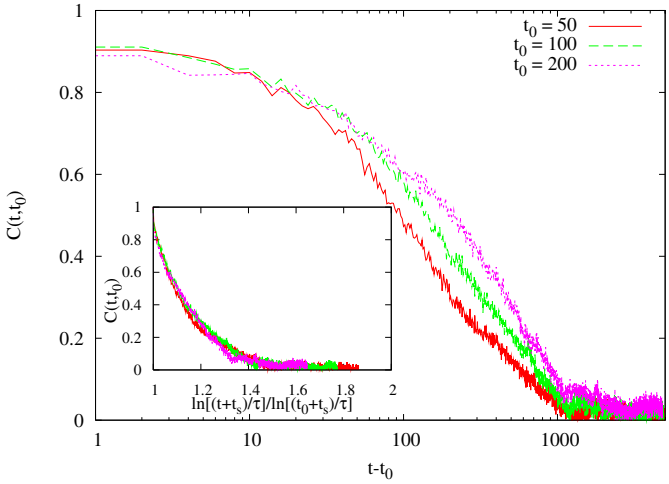

Fig. 11. (Color online) Two-time density-density correlation function as a function of $t - t_0$, for three values of waiting time, $t_0 = 50$ (solid), 100 (dashed) and 200 (doted). Other parameters: $P_+ = 1$, $P_- = 0.01$, and $P_d = 0$. Inset: The correlation $C(t, t_0)$ as a function of the scaling variable $\alpha = \ln[(t_0 + t_s)/\tau]/\ln[(t + t_s)/\tau]$. Fit parameters are $t_s = 210$ and $\tau = 8.0$.

where τ, t_s and c_∞ are fit parameters. The above behavior is found in our model. The inset of Figure 11 illustrates that when the two-time correlation function $C(t, t_0)$ is plotted as a function of $\ln[(t_0 + t_s)/\tau]/\ln[(t + t_s)/\tau]$ the data for three waiting times, $t_0 = 50$, 100 and 200, collapse onto single curve. This figure clearly demonstrates the existence of the single universal master function.

4 Concluding remarks

We have studied the density evolution of a granular system subjected to a tapping process in the framework of

a two-dimensional reversible RSA model with diffusional relaxation. Our model is a lattice based model, and in this sense it is not a realistic microscopic model of granular materials, but it does reproduce the complex phenomenology of granular media.

We have studied the response of a vibrated granular system to an instantaneous change in the intensity of the vibrations. The change in the compaction rate for a short time has an opposite sign to the one of the change in the vibration intensity. These results are in qualitative agreement with experimental observations [4].

Following reference [4], we have considered a series of numerical experiments where the system was compacted to ρ_0 using three different accelerations. After the density ρ_0 was achieved, the system was vibrated with the same intensity. These experiments indicate that the global density does not represent a good parameter for the description of a static packing, because the future evolution of density depends not only on ρ_0, but also on the previous tapping history. This additional feature lies in the coding of the system history by topological properties of the covering. We find that the coverings with the same density but reached with different compaction procedures may have completely different values of insertion probability. The numerical experiments have confirmed that the systems with different values of the insertion probability respond in a different way to abrupt changes in tapping intensity.

Recently, Tarjus and Viot [10,11] have applied the statistical mechanical approach proposed by Edwards and co-workers [28,29] to the parking-lot model, a one-dimensional model that reproduces the memory effects of the compaction of a vibrated powder. In their approach, a macrostate of the system is characterized by fixed values of three extensive parameters: the number of particles, the system size and the total length available for insertion of particles. They have postulated that all configurations (microstates) of nonoverlapping hard rods characterized by fixed values of density ρ and the available line fraction Φ are equally probable. The choice of Φ as an additional 'thermodynamic' parameter was crucial for reproducing various memory effects observed in parking-lot model. Our two-dimensional simulations have confirmed that the inclusion of the second state variable Φ is directly relevant for describing the history-dependent phenomena.

In addition we have studied the relevance of the diffusion in the process of granular compaction. The response of the system to a change in diffusion probability P_d is 'normal', in the sense that an increase in P_d produces a positive jump in the compaction rate. Such behavior shares some similarities with the phenomena of relaxation in vibrated *anisotropic* granular materials [3] (see Fig. 3 in [3]). During the compaction of the anisotropic granular materials there is an abrupt increase in packing fraction, which becomes less steep and smaller as Γ increases. This increase in the packing fraction coincides with the nematic ordering of the material. We have obtained similar effects by an abrupt change in diffusion probability (see Figs. 8 and 9).

We have also investigated the decay of density correlations. For our model we have observed a two-step relaxation of the density-density correlation function, which is a very common behavior in glassy systems. The first ('fast') relaxation step strongly depends on the diffusion probability.

Equation (2) leads to the conclusion that, for the long enough times, $C(t,t_0)$ is a function of the ratio $\ln(t_0)/\ln(t)$. Such scaling behavior is in agreement with the Ising frustrated lattice gas model and the Tetris model [13], but in contrast with the parking lot model [9], for which t/t_0 behavior has been observed. This finding suggest that the important step would be to relate the macroscopic dynamics of the compaction process to evolution of 'microscopic' structure of the packing experimentally [30].

The two-dimensional model presented in this work can be generalized to mixtures of several kinds of grains [31]. This allows us to study the compaction process in *polydisperse* granular systems under vibratory excitation.

This work was supported by the Serbian Ministry of Science and Technology under project 'Dynamical and Thermodynamical Properties of Strongly Correlated Systems with Complex Structures' (No. 1895). S.V thanks MNTRS (No. 1478) for financial support.

References

1. J.B. Knight, C.G. Fandrich, C.N. Lau, H.M. Jaeger, S.R. Nagel, Phys. Rev. E **51**, 3957 (1995)
2. E.R. Nowak, J.B. Knight, E. Ben-Naim, H.M. Jaeger, S.R. Nagel, Phys. Rev. E **57**, 1971 (1998)
3. F.X. Villarruel, B.E. Lauderdale, D.M. Mueth, H.M. Jaeger, Phys. Rev. E **61**, 6914 (2000)
4. C. Josserand, A. Tkachenko, D.M. Mueth, H.M. Jaeger, Phys. Rev. Lett. **85**, 3632 (2000)
5. M. Nicolas, P. Duru, O. Pouliquen, Eur. Phys. J. E **3**, 309 (2000)
6. J. Talbot, G. Tarjus, P. Viot, Phys. Rev. E **61**, 5429 (2000)
7. A.J. Kolan, E.R. Nowak, A.V. Tkachenko, Phys. Rev. E **59**, 3094 (1999)
8. J. Talbot, G. Tarjus, P. Viot, J. Phys. A: Math. Gen. **32**, 2997 (1999)
9. J. Talbot, G. Tarjus, P. Viot, Eur. Phys. J. E **5**, 445 (2001)
10. G. Tarjus, P. Viot (e-print `arXiv:cond-mat/0310738`)
11. G. Tarjus, P. Viot, Phys. Rev. E **69**, 011307 (2004)
12. M. Nicodemi, Phys. Rev. Lett. **82**, 3734 (1999)
13. M. Nicodemi, A. Coniglio, Phys. Rev. Lett. **82**, 916 (1999)
14. A. Baldassarri, S. Krishamurthy, V. Loreto, S. Roux, Phys. Rev. Lett. **87**, 224301 (2001)
15. A. Fierro, M. Nicodemi, A. Coniglio, Phys. Rev. E **66**, 061301 (2002)
16. A. Barrat, V. Loreto, J. Phys. A: Math. Gen. **33**, 4401 (2000)

17. A. Barrat, V. Loreto, Europhys. Lett. **53**, 297 (2001)
18. J.J. Brey, A. Prados, B. Sanchez-Rey, Phys. Rev. E **60**, 5685 (1999)
19. J.J. Brey, A. Prados, B. Sanchez-Rey, Physica A **275**, 310 (2000)
20. A. Prados, J.J. Brey, B. Sanchez-Rey, Physica A **284**, 277 (2000)
21. J.J. Brey, A. Prados, Phys. Rev. E **63**, 061301 (2001)
22. A. Prados, J.J. Brey, Phys. Rev. E **66**, 041308 (2002)
23. J.W. Evans, Rev. Mod. Phys. **65**, 1281 (1993)
24. G. Tarjus, P. Schaaf, J. Talbot, J. Chem. Phys. **93**, 8352 (1990)
25. L.J. Budinski-Petković, U. Kozmidis-Luburić, A. Mihailović, Physica A **293**, 339 (2001)
26. L.J. Budinski-Petković, T. Tošić, Physica A **329**, 350 (2003)
27. P.L. Krapivsky, E. Ben-Naim, J. Chem. Phys. **100**, 6778 (1994)
28. S.F. Edwards, D.V. Grinev, Phys. Rev. E **58**, 4758 (1998)
29. A. Mehta, S.F. Edwards, Physica A **157**, 1091 (1989)
30. O. Pouliquen, M. Belzons, M. Nicolas, Phys. Rev. Lett. **91**, 014301 (2003)
31. L.J. Budinski-Petković, U. Kozmidis-Luburić, Phys. Rev. E **56**, 6904 (1997)